Solar-blind ultraviolet photodetectors based on superlattices of AlN/AlGa(In)N

V. Kuryatkov, A. Chandolu, B. Borisov, G. Kipshidze, K. Zhu, S. Nikishin,[a] and H. Temkin
Department of Electrical and Computer Engineering and Nano Tech Center, Texas Tech University, Lubbock, Texas 79409

M. Holtz
Department of Physics and Nano Tech Center, Texas Tech University, Lubbock, Texas 79409

(Received 12 August 2002; accepted 7 January 2003)

We describe solar-blind photodetectors based on superlattices of AlN/AlGa(In)N. The superlattices have a period of 1.4 nm, determined by x-ray diffraction, and an effective band gap of 260 nm measured by optical reflectivity. Using simple mesa diodes, without surface passivation, we obtain low dark leakage currents of 0.2–0.3 pA, corresponding to the leakage current density of ~0.3 nA/cm^2, and high zero-bias resistance of $\sim 1\times 10^{11}\ \Omega$. Excellent visible cutoff is obtained for these devices, with six orders of magnitude decrease in responsivity from 260 to 380 nm. These results demonstrate the potential of junctions formed by short-period superlattices in large-band-gap devices. © *2003 American Institute of Physics.* [DOI: 10.1063/1.1557325]

High performance $p-i-n$ photodetectors, based on AlGaN, having high responsivity at ~280 nm have been demonstrated in the last few years.[1–7] These ultraviolet-sensitive detectors do not respond to the visible solar spectrum, and are known as solar-blind. Large-band-gap AlGaN, with more than 40% of AlN, is needed to obtain optical sensitivity in the desired region of the ultraviolet spectrum. Formation of $p-n$ junctions in such AlGaN layers remains very difficult, since the introduction and activation of *p*-type dopant (Mg) is increasingly difficult with higher AlN mole fraction.[8,9] We have shown recently that superlattices (SLs) based on AlN/AlGa(In)N, doped with Mg and Si, can be used to assure effective *p*- and *n*-type doping in structures with an average AlN content as high as 0.73.[10,11] This letter describes structural, electrical, and optical properties of SL-based $p-n$ junctions in order to demonstrate their potential as solar-blind photodetectors. Good results are obtained with simple device fabrication and without detailed structure optimization.

Device structures were grown on sapphire substrates using gas source molecular beam epitaxy with ammonia.[10,11] The device structure consists of a 40-nm-thick AlN nucleation/buffer layer deposited on sapphire, followed by a ~1-μm-thick Si-doped GaN buffer layer, two *n*- and *p*-type AlN/AlGa(In)N SLs and 10-nm-thick $Al_{0.08}Ga_{0.092}(In)N$:Mg contact layer. Each *n*- and *p*-type SL consisted of 150 pairs of $Al_{0.08}Ga_{0.92}(In)N$ quantum wells, 0.5-nm thick, separated by ~1.0-nm-thick barriers of AlN. Because of the high growth temperature of ~800 °C, the InN content in the wells was quite low, approximately 10^{17} cm^{-3}, as shown by secondary ion mass spectrometry (SIMS) measurements. Addition of small amounts of In improves the optical properties of SLs,[10,11] but the amount is too small to alter either the band gap or the period.

The *n*-type SL was doped with Si derived from silane. The *n*-type doping process is very effective and the dopant was introduced only during the growth of AlGa(In)N wells. The average Si concentration in the *n*-type SL, measured by SIMS, was $\sim 10^{20}$ cm^{-3}. Hall measurements yielded an electron concentration $n \sim 3\times 10^{19}$ cm^{-3}, consistent with the 30% room-temperature activation efficiency expected from the 30-meV donor depth of Si in GaN.[12] This result is also consistent with a recent report of highly doped *n*-type AlN/GaN SLs.[13] SIMS measurements of *p*-type SLs showed the average Mg concentration of $\sim 3\times 10^{19}$ cm^{-3}. Hall measurements on test SL structures with similar Mg concentration showed hole concentrations of $(2-3)\times 10^{17}$ cm^{-3} and mobilities of 5–8 cm^2/V s at room temperature.

The average AlN content and the period of our SLs were determined by x-ray diffraction (XRD). Figure 1 shows a (0002) rocking curve obtained on the SL-based photodetector structure. The GaN reflection is due to the ~1-μm-thick buffer layer. The thin nucleation layer of AlN contributes a broader and weaker peak. The AlN/AlGa(In)N SL produces a well-defined zero-order reflection peak consistent with an average AlN content of 0.63. The satellite peaks of SL, denoted +1 and −1, are also clearly seen. The average SL period is calculated to be 1.42 ± 0.05 nm. This is in excellent agree-

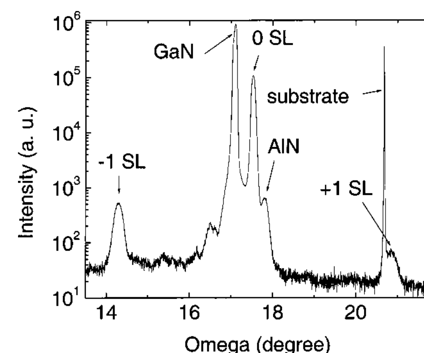

FIG. 1. XRD rocking curve of the SL photodetector structure grown on sapphire substrate.

[a]Author to whom correspondence should be addressed; electronic mail: Sergey.Nikishin@coe.ttu.edu

 © 2003 American Institute of Physics
Downloaded 10 Aug 2003 to 129.118.86.46. Redistribution subject to AIP license or copyright, see http://ojps.aip.org/aplo/aplcr.jsp

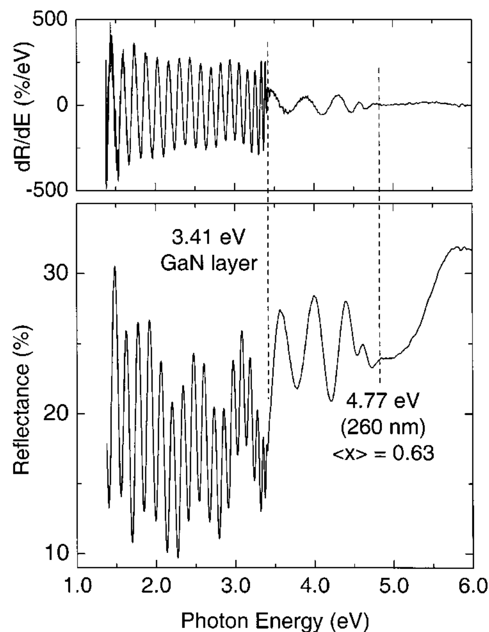

FIG. 2. Optical reflectance spectrum of the photodetector wafer (lower panel) and the derivative spectrum (upper panel).

ment with transmission electron microscopy measurement, which shows the SL period to be 1.42 ± 0.05 nm and the well/barrier thicknesses ratio of 0.67 ± 0.06. The zeroth SL reflection is somewhat broadened, suggesting that about 15% of the barrier/well pair periods may have monolayer variations from the design goal of 1.5 nm. The weaker structures near $\theta\sim15.4°$ and 16.6° are attributed to InN and GaInN, respectively. Their presence may indicate some degree of phase separation in the wells, despite low average concentration of indium.

The energy gap of the SL structure was obtained from reflectance measurements.[14] The lower panel of Fig. 2 shows the reflectance spectrum from the entire photodetector structure. The thin AlGa(In)N:Mg contact layer is not detected in the spectrum. Regularly spaced Fabry–Perot fringes are seen for photon energies below 3.41 eV. The disappearance of this fringe series is best seen in the derivative spectrum (upper panel) because it discriminates against gradual variations in the reflectance spectrum. These fringes have spacing associated with the total thickness of the epitaxial layers on sapphire substrate, ~1.73 μm. The closely spaced fringes disappear above 3.41 eV, the energy gap of GaN, and we see a separate series of fringes with larger periodicity (present as

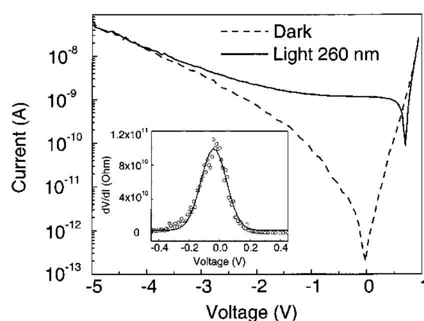

FIG. 3. Current–voltage characteristics of a photodiode in the dark (dashed line) and under 260-nm illumination (solid line). The inset shows differential resistance of the junction as a function of bias.

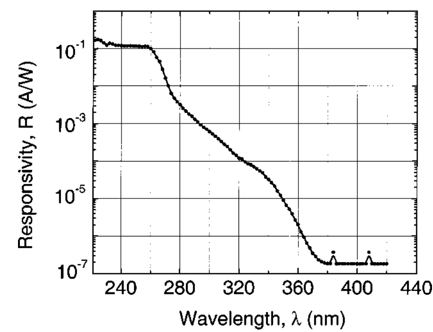

FIG. 4. Spectral responsivity of AlN/AlGa(In)N photodiode measured at zero bias under front illumination.

an envelope below 3.41 eV). These fringes are consistent with the total SL thickness ~0.434 μm, so that the GaN buffer layer is ~1.3-μm thick. The fringes exhibiting greater separation are associated with the SL and the optical gap at 4.77 eV (260 nm) is obtained from the disappearance of fringes in the derivative spectrum. This energy gap implies an average AlN mole fraction of 0.63 in the SL,[14] in excellent agreement with our x-ray measurements.

Mesa photodiodes were prepared using standard processing. The 280-μm-diameter mesas were reactive-ion plasma etched with Cl_2 using 100-nm-thick Ni masks formed by lift-off.[6,15] The Ni mask was stripped off after etching using a solution of HNO_3 and HF (10:1), at room temperature. *P*- and *n*-type contacts were processed separately. Contacts to *p*-type SL were made using 50 nm of Ni followed by 70 nm of Au. *N*-type contacts were made using Ti/Al/Ti/Au with a total thickness of 200 nm. High *p*-and *n*-type concentrations in as-grown layers make it possible to prepare Ni/Au and Ti/Al/Ti/Au ohmic contacts without activation anneals.

Current–voltage characteristics representative of our diodes are plotted in Fig. 3. Very low dark leakage currents, 0.2–0.3 pA, are measured near zero bias. For a mesa diode of 280 μm in diameter, this corresponds to the leakage current density of ~0.3 nA/cm^2. The reverse leakage current remains below 50 nA up to a bias of -5 V. Lower leakage currents can be obtained by introducing surface passivation of the mesa and introduction of an *i*-region.[7,16] The capacitance–voltage measurements of mesa diodes showed hole concentration in the *p*-type SL of $p\sim3\times10^{17}$ cm^{-3}, consistent with the Hall data.

From the (dV/dI) shown in inset of Fig. 3, we can calculate the zero-bias photodetector resistance of $\sim1\times10^{11}$ Ω, resulting in the area–resistance product R_oA $\sim6.2\times10^8$ Ω cm^2. The photodiode exhibits excellent photoresponse at zero bias, as shown in Fig. 3.

Spectral responsivity measurements were done at zero bias using a high-ultraviolet-output xenon lamp as a light source and a monochromator. Light intensity was measured using a commercial calibrated detector. The responsivity spectrum is shown in Fig. 4. The peak response was obtained at a wavelength of ~260 nm, in excellent agreement with the band gap of the SLs obtained by reflectivity measurements. The detector response at 260 nm was found to be linear over at least three orders of magnitude of the incident light power.

The detector responsivity does not fall off above the band gap, indicating low surface recombination velocity. Since the carriers are created close to the surface and must

Downloaded 10 Aug 2003 to 129.118.86.46. Redistribution subject to AIP license or copyright, see http://ojps.aip.org/aplo/aplcr.jsp

diffuse to the junction in order to be collected, this also indicates minority carrier (electron) diffusion length greater than ~200 nm, the thickness of the *p*-type SL. Responsivity decreases below 260 nm, and it drops off by almost six orders of magnitude at 380 nm, showing an excellent rejection of radiation in the visible. This compares well with the rejection ratio of four orders of magnitude in state-of-the-art conventional $p-i-n$ detectors.[17] The substructure visible in the photoresponse in the range of ~280–340 nm is not understood at this time. It may be partially related to absorption in the exposed GaN buffer layer, at the bottom of the device mesa, but this would imply fairly long hole diffusion lengths. Another possibility is the broadening of the absorption edge due to monolayer thickness fluctuations in the well and barrier thickness. We plan to answer some of these questions by growing additional SL structures on AlN buffer layers.

Responsivity of 25 mA/W was measured at wavelength of 260 nm. This corresponds to an external quantum efficiency of 12.5%. This is less than the highest responsivity reported in solar-blind $p-i-n$ detectors of ~42%.[7] However, our present device does not have an *i*-layer and the *p*-type SL is used as the absorbing region, resulting in lower efficiency. In addition, our device is top illuminated and external quantum efficiency is decreased by absorption in the contact layer. Nevertheless, using the R_oA determined previously, we calculate the thermal noise-limited specific detectivity, at zero-bias, of $D^* = 1.4\times10^{12}\ \mathrm{cm\,Hz^{1/2}\,W^{-1}}$. Introduction of an *i*-layer is expected to improve quantum efficiency and to result in improved D^*.

In summary, we have prepared solar-blind photodetectors based on short-period SLs of AlN/AlGa(In)N. Excellent electrical characteristics of $p-n$ junctions formed in these SLs demonstrate their potential in large-band-gap photodetectors.

Work at Texas Tech University is supported by DARPA, NSF (ECS-0070240 and ECS-9871290), SBCCOM, NATO-Science for Peace, and the J. F. Maddox Foundation. The authors are grateful to Dr. G. A. Seryogin for x-ray measurements, Dr. S. N. G. Chu for transmission microscopy measurements, and Dr. Yu. Kudryavtsev for SIMS measurements.

[1] J. D. Brown, J. Li, P. Srinivasan, and J. F. Schetzina, MRS Internet J. Nitride Semicond. Res. **5**, 9 (2000).
[2] C. Pernot, A. Hirano, M. Iwaya, T. Detchprohm, H. Amano, and I. Akasaki, Jpn. J. Appl. Phys. **39**, L387 (2000).
[3] V. V. Kuryatkov, H. Temkin, J. C. Campbell, and R. D. Dupuis, Appl. Phys. Lett. **78**, 3340 (2001).
[4] A. Hirano, C. Pernot, M. Iwaya, T. Detchprohm, H. Amano, and I. Akasaki, Phys. Status Solidi A **188**, 293 (2001).
[5] G. Parish, M. Hansen, B. Moran, S. Keller, S. P. DenBaars, and U. K. Mishra, Phys. Status Solidi A **188**, 297 (2001).
[6] V. V. Kuryatkov, G. D. Kipshidze, S. A. Nikishin, P. W. Deelman, and H. Temkin, Phys. Status Solidi A **188**, 317 (2001).
[7] C. J. Collins, U. Chowdhury, M. M. Wong, B. Yang, A. L. Beck, R. D. Dupuis, and J. C. Campbell, Appl. Phys. Lett. **80**, 3754 (2002).
[8] L. Akasaki and H. Amano, *Gallium Nitride (GaN)*, edited by J. I. Pankove and T. D. Moustakas (Academic, San Diego, 1998), pp. 459–472.
[9] J. Li, T. N. Oder, M. L. Nakarmi, J. Y. Lin, and H. X. Jiang, Appl. Phys. Lett. **80**, 1210 (2002).
[10] G. Kipshidze, V. Kuryatkov, B. Borisov, M. Holtz, S. Nikishin, and H. Temkin, Appl. Phys. Lett. **80**, 3682 (2002).
[11] G. Kipshidze, V. Kuryatkov, B. Borisov, S. Nikishin, M. Holtz, S. N. G. Chu, and H. Temkin, Phys. Status Solidi A **192**, 286 (2002).
[12] W. J. Moore, J. A. Freitas, G. C. B. Braga, R. J. Molnar, S. K. Lee, K. Y. Lee, and I. J. Song, Appl. Phys. Lett. **79**, 2570 (2001).
[13] S. Yamaguchi, Y. Iwamura, Y. Watanabe, M. Kosaki, Y. Yukawa, S. Nitta, S. Kamiyama, H. Amano, and I. Akasaki, Appl. Phys. Lett. **80**, 802 (2002).
[14] M. Holtz, T. Prokofyeva, M. Seon, K. Copeland, J. Vanbuskirk, S. Williams, S. A. Nikishin, V. Tretyakov, and H. Temkin, J. Appl. Phys. **89**, 7977 (2001).
[15] K. Zhu, V. Kuryatkov, B. Borisov, G. Kipshidze, S. A. Nikishin, H. Temkin, and M. Holtz, Appl. Phys. Lett. **81**, 4688 (2002).
[16] P. W. Deelman, R. N. Bicknell-Tassius, V. V. Kuryatkov, S. A. Nikishin, and H. Temkin, Appl. Phys. Lett. **78**, 2172 (2001).
[17] P. Sandvik, K. Mi, F. Shahedipour, R. McClintock, A. Yasan, P. Kung, and M. Razeghi, J. Cryst. Growth **231**, 366 (2001).

Downloaded 10 Aug 2003 to 129.118.86.46. Redistribution subject to AIP license or copyright, see http://ojps.aip.org/aplo/aplcr.jsp